Design of an electromagnetic actuator to perturb the rabbit eye

Maria Dagioglou Department of Biomechanical Engineering TUDelft

January 22, 2010

Abstract

In order to understand how the different brain systems work, control theory concepts are used to represent the input - output relationships of the structures involved. Perturbations is a common tool to study and analyze a control system. One example of a brain circuitry is the oculomotor system. Although, visual perturbations have been used to perturb the eye no mechanical perturbations have been applied up to now. Mechanics is the only way to evoke an unexpected movement, which is an essential factor to motor control. In this study, a magnetic actuator is designed to be used to apply torques in the rabbit eye. In vitro experiments were conducted in a prototype, which roughly mimics the movement of the eye in the horizontal plane, to test the function of the actuator. Experiments in the rabbit (in vivo) were also performed. In vitro results showed that the conceptual design is sound and the demanded torque of 17 mN mm was achieved. During preliminary in vivo results, clear eye movements were recorded as a result of the actuator's perturbations. The actuator designed enables a series of experiments in the frame of oculomotor control research.

I Introduction

People move their eyes to read, to follow a bird flying in the sky, to focus at objects found at different distances and to compensate for head movements. Eye movements are feasible when the eye rotates under the action of extraocular muscles (EOM). Robinson [17] introduced the term oculomotor plant (OP) to refer to the physical plant to be controlled. Oculomotor control refers to how the brain actuates the eye muscles in order to move the OP. During the last decades a lot of research effort has been done in the field of oculomotor control. Research on oculomotor control has been of great value not only from a pure scien-

tific perspective but also for better comprehension of several pathological conditions, like strabismus [14], [24]. Moreover, better understanding of motor control, including oculomotor control, is closely related to the advance of engineering fields like robotics.

A highly disputable issue has been whether sensory nerve endings (receptors) in the EOM provide the brain information and thus act as proprioceptors. Proprioceptors provide feedback to Central Nervous System (CNS) about the state of the muscles, at least in the case of the limb muscles. Although the existence of proprioceptors in eye muscles has been a topic of research since the beginning of the 20th century [8]- through morphological (e.g. [15], [18]), physiological (e.g. [1]) and experimental (e.g. [24]) studiesevidence is not decisive. Another related question around this topic is what could be role of proprioceptors in the oculomotor control. Some studies suggest that proprioception in the eye muscles can influence visual attention [2]. Moreover, oculomotor proprioception is critical for long-term calibration of the motor system [26].

The role of the cerebellum in motor control [20], including oculomotor control, has also been a research question. It is widely believed that the cerebellum acquires and stores internal models of the motor apparatus [9]. These internal models provide representations of the input-output relation of the plant (or its inverse). By incorporating concepts from control theory, two possible control schemes were proposed to explain the use of internal models. Inverse models provide the motor commands that will cause a desired change in state [27], and thus act as feedforward control. On the other hand, a forward dynamic model predicts the state of the system, either the motor variables or the sensory output, as a consequence of the current state of the eve and the motor commands (Kalman filter) [16], [11]. Moreover, it has been proposed that the cerebellum could function as a paired forward and inverse model [27].

In order to identify the role of the cerebellum the nature of the input- output signal must be clarified. For example, is the source of the oculomotor signal found in the cerebellum a copy of the motor command (efference copy) sent to the OP or is it a sensory registration of the actual movement [25]? As far as the output of the cerebellar cortex is concerned, there is only one type of output cell, called Purkinje cell (P-cell). P-cells show two different kinds of electrophysiological activity: simple spikes (SS) and complex spikes (CS). The question that arises about SS and CS is whether they contain both motor and sensory components [16], [27].

Disturbance experiments that allow for system identification [25],[22],[7],[9] are the common performed strategy in answering questions like the ones posted above. Disturbance experiments are applied to joints with aid of a robotic manipulator [19] or by a moving platform to investigate balance control [23]. Static forces have been applied to human eyes [4], [6] and rabbit eyes [3] in research for the stiffness of the EOM. Sinusoidal torques were used to human eyes for the identification of the torque-angle transfer function of the human eye [21].

The goal of the current study is to develop an electromagnetic actuator suitable to apply torque disturbances to the rabbit eye. Although eyes do not need to compensate with such conditions in real life, recording of eye reaction to the perturbations, and also check for the coherence to the signals recorded in the cerebellum, gives a method to research on the topics mentioned above. Of the animals available for the experiments, rabbits have been chosen over mice because of the size of their eyes. To our knowledge, electromagnetic perturbations were applied only in [21] to human eyes. An electromagnetic actuation principle was chosen in order to prevent mechanical coupling between the eye and the device. This will allow the animal to blink his eyes, prevent injury due to (small) undesired movement between the eye and the device and accommodate relatively easy set up of the animal within the device.

The principal idea of the electromagnetic actuation principle was tested in a prototype, which roughly mimics the movement of the eye in the horizontal plane. The results from the prototype are used to define the specifications for the design for the rabbit eye actuator. Finally the feasibility of the actuator is tested in the rabbit.

II Materials and Methods

A Oculomotor system of the rabbit

The rabbit has laterally placed eyes. The monocular visual field has a total extension of 192^o in the horizontal field. Frontally, the visual fields of the two eyes overlap in a potentially binocular zone of a width of about 24^o [5]. Eye movements contribute mainly to the stability of eye position in visual space. On contrary, human eyes are placed frontally, with a binocular zone of 180^o . Human eye movements do not account only for the stability of the eye position, but also for the clear vision. The target of the eye movements is to place the area of interest in the fovea. As a result human make many fast eye movements (saccades) while this is normally not seen in rabbits.

The only value found on literature concerning the stiffness of the rabbit eye is in [3]. In concrete, it is reported that:

"With all muscles attached to the globe, the stiffness of the eye for displacements of up to 35° from primary position was 0.11 ± 0.03 g/deg."[3]

The aforementioned value indicates that in order to rotate the eye by 1^o , 1mN force is demanded. Given that the rabbit eye can be considered as a sphere with a radius of 8.5 mm, the rotational stiffness is $4.9\,10^{-4}Nm/rad$. In high frequency perturbations, viscosity plays a significant role. There was no estimation found in the literature about viscosity and thus no safe assumption can be made a priori.

B Demands and Considerations

The demands about the device relate to the intended function of the device. Moreover, additional considerations must be taken into account. Those considerations concern the safety of the test animal, space limitations and interaction with surrounding devices that can be part of the experiments.

The device must able to exert torque perturbations to the rabbit eye. At first place, only the excitement of horizontal movements up to 2^o around the primary position is object of the design. Thus, the desired torque to rotate the eye is $17mN\ mm$. Two types of torque perturbations are desired; static torques under the effect of a static force field (SFF) and unpredictable torques with a bandwidth of $\approx 10 \text{Hz}$. The demands are summarized in Table 1.

In addition to the demands some extra aspects need to be considered. During some experiments the

Table 1: Demands of the actuator

Movement	Horizontal
Range of movement	$\pm 2^{o}$
Max. Torque	$17mN\ mm$
Torques	1)Static (SFF)
	2)Unpredicted (BW=10Hz)

animal will be placed on the top of a rotation table. The size of the device should satisfy the limitations imposed by the rotating table where the device will be attached. The radius of the rotating table is around 20cm and the rabbit occupies around 20% of it. Furthermore, during the experiments a pupil detection infrared camera will be placed in front of the eye. This poses limitation in the position of the device as the vision of the animal should not be blocked. Electromagnetic interference (EMI) could impose unwanted signals to circuits of the camera causing alteration of the data captured and must be avoided. The additional inertia by any components of the actuator placed in the eye must be minimal. Last but not least, the device should not by any means harm the eye and the animal.

C Theoretical background

C.1 Magnetic field of a circular coil

When an electric current flows in a wire a magnetic field is generated. The Biot-Savart law is used to calculate the magnetic field intensity as a function of the current that generates it. According to the Biot-Savart law, in a circular coil with current i passing through, the intensity of the magnetic field along the center of the coil is [12]:

$$H_z = \frac{Nir^2}{(r^2 + z^2)^{\frac{3}{2}}} \tag{1}$$

where r is the radius and N the number of the coil windings. The subscript z of H is the axial coordinate when the center is zero. As follows from equation (1), the magnetic field intensity generated by the coil is directly proportional to the current intensity and inverse proportional to z^3 .

C.2 Force on a permanent magnet in a non-homogeneous field

A permanent magnet (PM) can be considered as an array of dipoles, each with magnetic moment \mathbf{m} , oriented in the same direction. The magnetization \mathbf{M} of a PM of volume V equals to \mathbf{M} = \mathbf{m} dV.

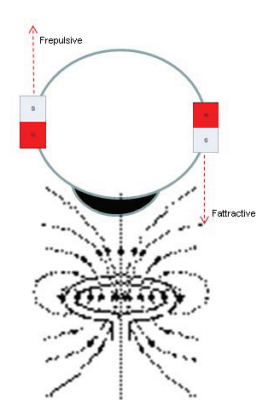


Figure 1: Conceptual design: Top-view of the eye. Two permanent magnets are placed laterally with opposite orientation. If those magnets are in a magnetic field, an attractive and repulsive force will be developed, producing a torque.

The total force on a PM in a nonhomogeneous field with flux density $\mathbf{B}=\text{mo}\mathbf{H}$ is [13]:

$$F_z = \int_{\mathbf{s}} (\mathbf{M} \cdot \mathbf{B}) d\mathbf{S} \tag{2}$$

where $d\mathbf{S}$ is a vector in the surface normal direction.

Substituting the magnetic field intensity \mathbf{H} of equation (1) in equation (2), the force exerted on a PM in a field \mathbf{B} , produced by a coil, is given. The force F_z is directly proportional to current i. Moreover, the magnetic field increases with decreasing radius of the coil. Thirdly, F_z is implicitly independent of the number of the turns of the coil for constant electric power P [10].

D Conceptual design

If a permanent magnet is found inside the magnetic field created by a coil, based on equation 2, a force F_z will result. Let us suppose that a permanent magnet is implanted in the rabbit eye which has a radius R_{globe} . Under the influence of an external magnetic field a torque $T = F_z R_{globe}$ will rotate the eye.

Moreover, F_z would also translate the eye globe towards outside (or inside depending on the orientation of the field), even though the restriction of the globe by the orbit makes that unlikely. When two magnets would be implanted in the rabbit eye at the sides across the midline with different orientation, these translational forces are compensated and the effective torque will be doubled. A schema to illustrate this conceptual design is shown in Figure 1.

As the eye rotates one magnet approaches the coil, while the other departs away from it. Since the field of the coil is not homogeneous, described by equation 1, the attractive force will increase, while the repulsive force decreases. For large rotations, this behavior could cause forces in other direction than the desired thus causing unwanted movements (e.g. horizontal translations). However, the small rotations demanded (2^o) are a safety margin to assure that the two forces have more or less the same magnitude and force components in other direction will be negligible.

E Choice of permanent magnets

In selecting the appropriate permanent magnets (PMs) to be implanted, there were two main considerations. First of all, the volume and the geometry of the PM is firmly related to its power. As a general rule the bigger the volume the strongest it is. Moreover, two PMs with the same volume but different geometry could differ in strength.

On the other hand, the size of the PMs should comply with the anatomy of the globe of the rabbit eye, which on average is a sphere of 17mm diameter. Once implanted in the eye the width of the magnet should be as small as possible. It was decided that the width should not exceed 1 mm. Thus, the geometry that would give the maximum magnetic strength given the space limitations was chosen. Neodymium iron boron magnets of size of 5x1.5x1 mm (magnetization N45) were selected.

F Set up

To test the principle presented in paragraph D the device shown in Figure 2 was developed. The characteristics of the set-up are summarized in Table 2. A ring with radius R_{ring} =15mm was allowed to rotate around the vertical axis under the constriction of two bearings. The material used for the device was PVC as to avoid any electromagnetic interaction with the PMs and the coil.

At the sides of the ring two permanent magnets (PMs) were placed. The PMs were the same as the ones that were chosen to be implanted to the rabbit eye. The orientation of the two magnets was opposite. Moreover, the distance between the magnets in the set up was around 17mm.

Two elastic bands of stiffness 10mN/mm were attached at each side of the ring. The other end was anchored in hooks at two load cells¹. The load cells

Table 2: Technical characteristics of the set-up

Ring radius R_{ring}	15mm	
Coil radius R_{coil}	12.5mm	
PMs	5x1.5x1 mm	
	distance=17mm	
Elastic bands' Stiffness	$k_{el} 10 \text{mN/mm}$	
Coils' ohmic resistances	$R_{200} = 4.8\Omega$	
	$R_{300} = 7.4\Omega$	
	$R_{400} = 10.8\Omega$	
	$R_{500} = 13.3\Omega$	

allowed registration of the forces developed as a result of the interaction of the magnetic field of the coil and the PMs. The range of forces that could be recorded was between 1mN to 2N.

The signals from the load cells were directed to two Analog Signal Conditioners (ASC) ². The output voltage of the ASCs was connected with a 16-bit Data Acquisition device (DAQ)³. The signals were recorded with LABview.

The coil was placed opposite to the ring with the PMs, at a distance of around 8mm. The radius of the coil was R_{coil} =12.5mm. That was a choice made considering what the minimum diameter is, given that the pupil of the eye should not be obscured.

Four different custom-made coils of 200, 300, 400 and 500 windings were used. The coils were made with copper wire of 0.3mm diameter. The resistance of the coils were $R_{200}=4.8\Omega,\ R_{300}=7.4\Omega,\ R_{400}=10.8\Omega$ and $R_{500}=13.3\Omega.$

By recording the mechanical forces developed at each band we could implicitly measure the torques developed by the coil and the PMs.

G Experiments

G.1 Static torques with DC current

The purpose of this set of experiments was at first place to check if the main principle of the conceptual design was sound. Once that was proven the appropriate coil had to be defined and the magnetic field in which the permanent magnets should be placed had to be specified. Since the radius of the coil R_{coil} was chosen considering the rabbit eye, the strength of the magnetic field depends on the applied current and consequently the power.

The first criterion to decide about the level of power P was the magnitude of forces provoked at

 $^{^1\}mathrm{Load}$ Cells: PW4C3/300G of HBM

 $^{^2\}mathrm{CPJ\text{-}CPJ2S}$ from SCAIME

³NI USB-6211

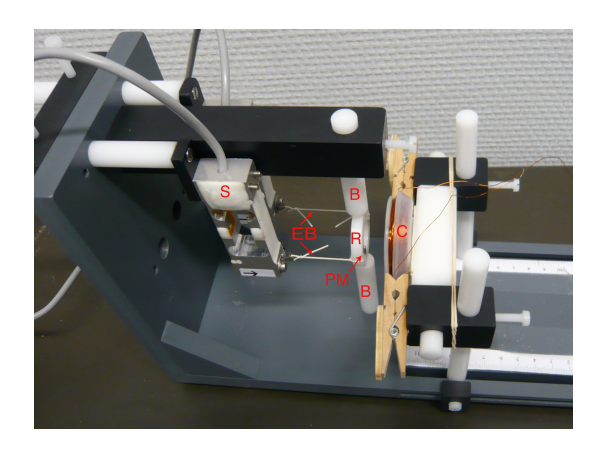


Figure 2: The set-up: the ring (R) was allowed to rotate around the vertical axis under the constriction of two bearings (B). Two permanent magnets (PM) were placed at the sides of the ring. The sides of the ring were connected through elastic bands (EB) to the load cells (S). Finally, the coil (C) was placed opposite to the ring.

each level. The power was calculated as $P = I^2 R_{coil}$, where I was the current in the coil. Each coil was conducted, in discrete steps, by currents of 0.5, 1, 1.5 and 2 A. The force generated in each case was recorded. Following, the power in each condition was calculated taking into account the ohmic resistances. Thus, the forces were related with the power level that was bringing them about. Moreover, the net torque at each case was calculated as $T_{net} = (F_{left} - F_{prestress})R_{ring} - (F_{right} - F_{prestress})R_{ring}$, where $F_{prestress}$ is the prestress at each elastic band, F_{right} and F_{left} the forces at the right and left elastic band accordingly.

A second criterion was the temperature developed on the surface of the frame the coils were looped around. For this reason coils selected from the previous criterion, and only at selected currents, were tested. A thermocouple was used to measure the temperatures. The rise time up to 38° or 40° was recorded (that was usually the case of temperature being bearable by palpation). The time needed for the coils to cool down was also measured during this test, in order to define safety margins later.

Combining the two aforementioned criteria the final choice of the appropriate coil was made. The choice was a trade-off between the maximum torque that could be developed because of the magnetic field of a coil and the temperature produced on it. In other words, the coil should be able to be used as long as possible, while ensuring the development of desired torques. Finally, how the static torques are varied in dependence with the distance between the PMs and the coil were measured. Only one coil was used. The coil was placed, in steps of 1mm, 3-9mm away form the magnets. The distances were chosen to be around the operating point. Four different currents of 1.5, 1, 0.7 and 0.5A were used.

G.2 Dynamic behavior of the system coil-PMs

The goal of this set of experiments was to define the dynamic behavior of the system PMs - coil. The relationships defined in paragraphs C.1 and C.2 refer to the case that the field is static. So, it had to be tested what is the behavior of the system when the PMs are found in a AC magnetic field.

The coil was directly supplied by a function generator. The current amplitudes supplied by the function generator were too small and for this reason, the coil of 500 windings was used to achieve higher power. The distance between the coil and the permanent magnets was around 3mm. Ten different sinusoids were applied to the coil. Their frequencies varied between 1-10Hz, which is the bandwidth demanded for the unpredictable torques.

Due to limitations in the available equipment it was not possible to record the current in the coil, neither to amplify the current and keep it steady at each frequency. At each frequency the peak to peak voltage was read by an oscilloscope. The RMS current (I_{rms}) in the coil was calculated by diving the RMS value of the voltage by the impedance of the coil. It was considered that the coil is a series ohmic resistance of $R_{500}=13.3\Omega$ and an inductance of L=11.5mH. The inductance value was calculated by finding the resonance frequency $(f\simeq 1.2KHz)$ of a series circuit consisting of the coil and a $2.2\mu F$ capacitor.

G.3 Experiments on the rabbits

Once the principle was proved in-vitro, it had to be tested in the rabbits. The most important thing to be decided was how to implant the magnets in the eye. The two magnets were glued at the edges of a silver semi-ring as shown in Figure 3. Following, the semi-ring with the magnets was put in epoxy glue, in order to acquire biocompatible properties.

During the experiments, the coil was placed in front or the rabbit eye. An infrared camera recorded the eye movements (Figure 4). At this stage, only preliminary tests have been conducted to check if any movement is provoked, at all.



Figure 3: The Semi-ring and the two PMs. To be implanted in the rabbit eye.

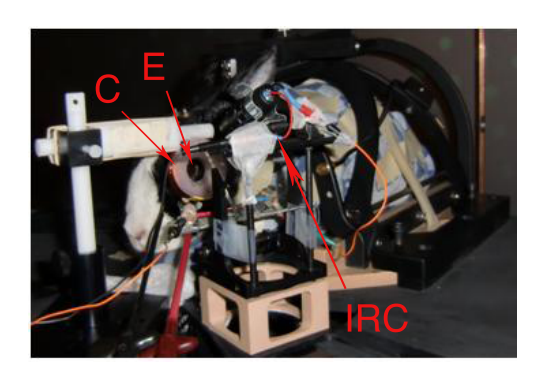


Figure 4: The coil (C) is placed in front of the rabbit eye (E). An infrared camera (IRC) is under the table and looks at the eye through a hot mirror (which you can see in the picture). The IRC arrow is directed to one of the IR LEDs.

The coil was placed around 7mm away from the rabbit. DC current of 0.7, 1.5 and 2A was applied at the coil. The application time was always short to avoid excessive heating.

III RESULTS

A Static torques with DC current

A.1 Forces, Torques and Power

Figure 5 presents the forces in the elastic bands, as recorded by the sensors, depended on the current applied to the coils. Four different cases are presented, each corresponding to the four different coils with 200, 300, 400, and 500 windings accordingly. For each coil, the forces developed in the right and left elastic band are shown. The increasing force in the right elastic band and the decreasing force in the left, indicate the different magnetic force direction. At 0A the force denotes the pre-stress on the elastic bands. The difference between the pre-stress in the right and left elastic band was a result of the non identical starting value of the sensors, and perhaps a small mismatch in the moment arm. Although the technical characteristics of the two sensors were the same, it was

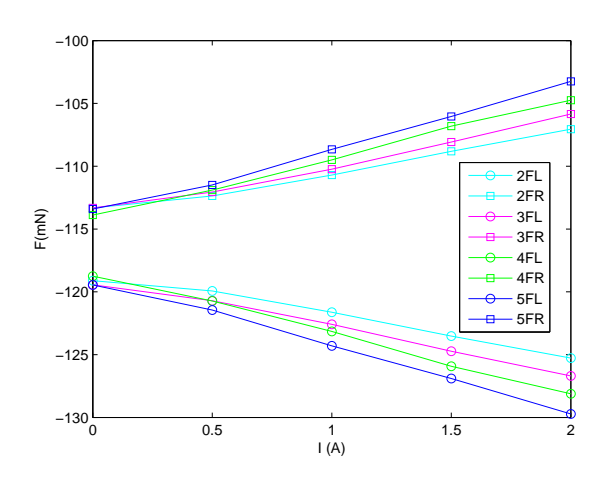


Figure 5: Forces vs Current: Four coils of 200 (cyan), 300(magenta), 400(green) and 500 (blue) windings were used. The force in the right (FR) and left (FL) elastic band was recorded. The currents used were of 0.5, 1, 1.5 and 2 A. The force at 0A results from the pre-stress in the elastic bands.

impossible to achieve identical calibration. As it was expected the forces are linearly related to the current I, and thus to the magnetic field \mathbf{B} .

The torques developed in each case (of different current and different coil) are shown in Figure 6. The maximum torque achieved was around 300 mNmm. This value is 17 times higher than the desired value of 17 mNmm to rotate the eye $\pm 2^o$ around its primary position.

In Figure 7 the forces acting on both magnets are plotted versus the power P. The developed force by the interaction of the PM and the magnetic field of the coils are calculated by subtracting the pre-stress in the elastic bands. Moreover, two fit curves are plotted, corresponding to the forces in the right and left elastic band. The fit curves are almost the same with $F_{left}=1.346(P-0.8161)^{1/2}$ and $F_{right}=1.351(P-0.7821)^{1/2}$. The root mean squared error for both fit curves is 0.28.

The nice fit of the curves confirms that the all the repetitions were conducted under similar conditions as far as the distance of the coils compared to the permanent magnets is concerned.

A.2 Temperature on coils

The results of the measurements of temperature are summarized in Table 3.

The ambient temperature was difficult to be kept completely steady, and as a result the initial temper-

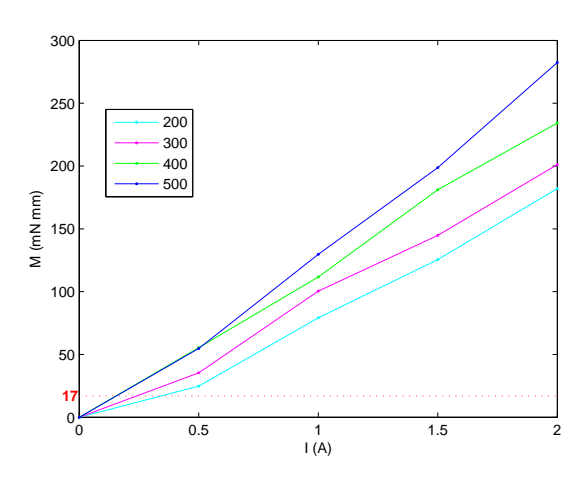


Figure 6: Torques vs Current: Four coils of 200 (cyan), 300(magenta), 400(green) and 500 (blue) windings were used. For each case the net torque is calculated. The currents used were of 0.5, 1, 1.5 and 2 A. The red dotted line indicates the demanded torque of 17mNmm.

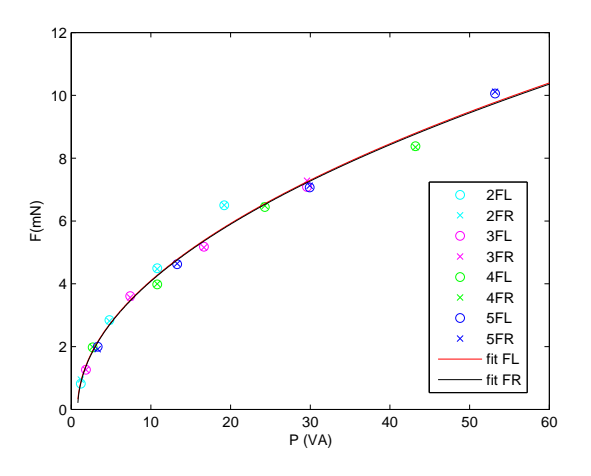


Figure 7: Forces vs Power: Four coils of 200 (cyan), 300(magenta), 400(green) and 500 (blue)loops were used. At each case the force in the right (FR)and left (FL) elastic band were calculated as $FR = |F_{right} - F_{prestress}|$ and $FL = |F_{left} - F_{prestress}|$. The power at each case is the product of the current times the ohmic resistance of each coil.

Table 3: Rising up time of temperature on the coils depending on the applied current.

Coil	I (A)	Time	T_{In}	T_{Fin}
300	1	1min 40sec	$22^{o}C$	$40^{o}C$
300	1.5	54sec	$22^{o}C$	$38^{o}C$
400	1	1min 25sec	$24^{o}C$	$40^{o}C$
400	1.5	45sec	$23^{o}C$	$38^{o}C$
500	1	1min 30sec	$22^{o}C$	$38^{o}C$
500	1.5	40sec	$21^{o}C$	$38^{o}C$

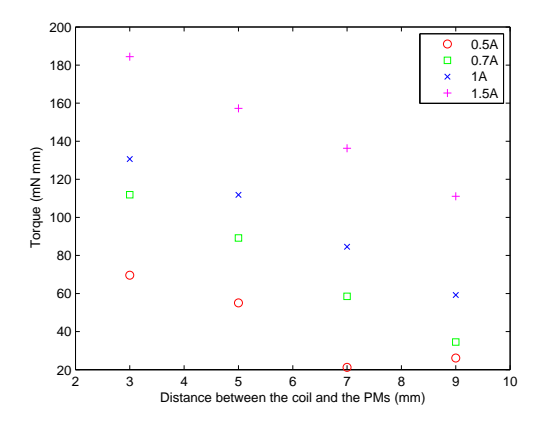


Figure 8: Torques vs Distance: The 400 windings coil was placed at several distances away for the PMs. The coil is placed 3-9mm (with steps of 2mm)away form the permanent magnets. The experiment was repeated four times with different currents.

atures T_{In} were not steady.

Moreover, the final temperature T_{Fin} was the temperature at which palpation of the coils' surface was bearable. Moreover, it is important to note that in each case the coils needed at least 5 minutes before they cool down.

A.3 Torques in dependence to the distance

Figure 8 shows that up to 9mm away from the magnets the torques relate linearly with the distance. This Figure allows us to make the assumption that in the area of interest the magnetic field can be considered to propagate in a relatively linear way.

B AC current passing through the coil

In Table 4 the peak to peak values of the voltage as read in the oscilloscope, the calculated RMS value of the current, as well as the RMS value of torque are given.

Table 4: Peak to peak voltage V_{p-p} (oscilloscope) , the calculated RMS value of the current I_{rms} , and RMS value of torque T_{rms} .

Frequency	V_{p-p}	I_{rms}	T_{rms}
(Hz)	(V)	(A)	(mNmm)
1	0.8	0.02	6
2	1.37	0.036	6
3	2	0.05	7
4	2.44	0.06	8
5	2.8	0.07	10
6	3.12	0.08	9
7	3.36	0.08	10
8	3.56	0.094	12
9	3.72	0.098	12
10	3.8	0.1	10

As shown in Table 4, the linear relationship between the current and the torque is in some cases violated (5 and 10Hz). This is most probably due to the discrepancies caused in the measurements because of the small forces (generated by small currents) and do not represent the properties of the system.

In Figure 9 the forces on the sensors and the net torque on the ring, in each frequency, are shown. We can conclude that the system is linear. However, from 1 to 5 Hz there are non linearities observed because of the friction. The currents applied to the coil are too small to generate forces large enough to overcome the effects of friction at all times.

C Experiments on the rabbits

10 days after implantation, the rabbit eye had recovered sufficiently. During, the preliminary trials, the experiment was successful. Clear eye movements were recorded by the infrared camera. In Figure 10 it is shown that every time current is applied to the coil the eye moves (peaks in voltage). When the voltage in the coil was inverted the movement changed orientation.

IV Discussion

A Principle and function of the actuator

The basic principle behind the design of the electromagnetic actuator is that if two magnets with different orientation, placed in the midline of the rabbit eye, are found in the magnetic field of the coil, the repulsive and attractive forces will create a rotation.

At first place it is checked if indeed the principle

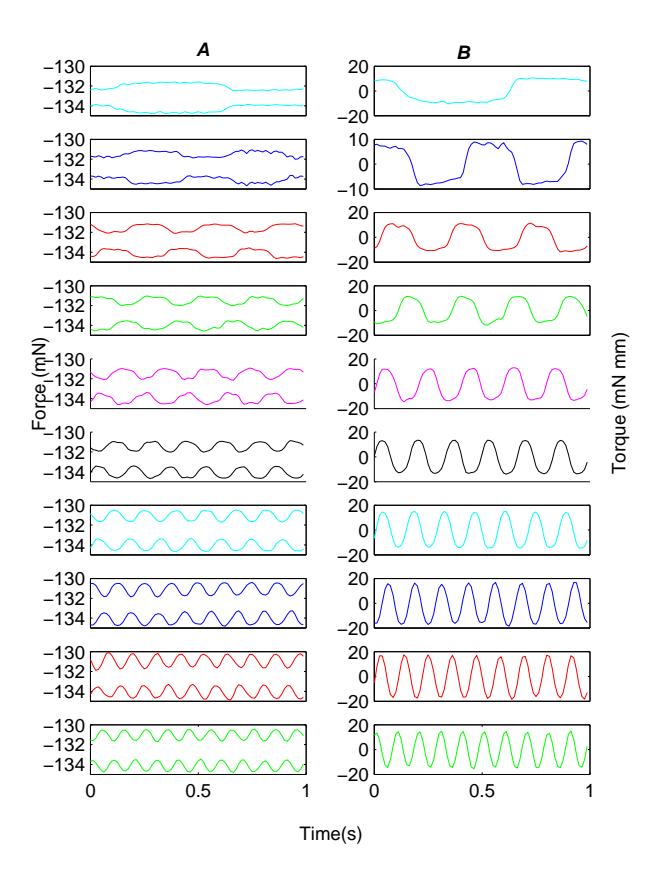


Figure 9: The output sinusoids: (A)Forces on the sensors and (B) the net torque on the ring (y-axis). The input frequency was from top to bottom 1 to 10Hz with steps of 1Hz. The measurements presented are over 1 second.

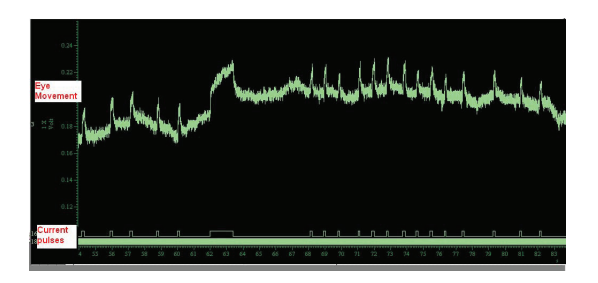


Figure 10: Recording of eye movements. The peaks change in voltage indicate a movement. Every time that current is applied to the coil the eye moves.

works. Figure 5 shows clearly that two forces with different direction are developed. Thus, an actuator to provoke torques is feasible with this topology of PMs and a coil. Moreover, the demand of provoking torques that would allow rotation of $\pm 2^{\circ}$ around the primary position of the eye is successfully met, as proved by Figure 6.

Commenting about the propagation of the magnetic field \mathbf{B} , Figure 8 can be used under the assumption that the torque is proportional to the magnetic field (see Appendix B for justification). It is shown that the field decays in a linear way.

Let us assume that the coil is fixed in a certain distance d away from the magnets. At first place, from equation 1 the magnets experience a magnetic field B_{in} proportional to $1/(r_{coil}^2 + d^2)^{3/2}$. After a rotation of $\theta = 2^o$ the magnetic field B_{fin} is proportional to $1/(r_{coil}^2 + (d - r_{eye} \sin \theta)^2)^{3/2}$. When the coil is near to the permanent magnets (e.g d=4-12 mm) then the change in magnitude of the magnetic field is in the order of 2%. As a result, $B_{in}/B_{fin} \approx 1$ and we can assume that also the force has the same magnitude. So, the static magnetic field remains stable over the rotations demanded.

Even if we take into consideration the small change in the field, given that it is linear, as discussed earlier, the repulsive and attractive forces in the eye will increase and decrease, accordingly, by the same magnitude. In any case we can say that the eye during small rotation experiences the same torque. In addition, following the same rationalization, the perpendicular forces that could cause unwanted horizontal translations, since they have approximately the same magnitude but different direction, they are compensated.

B Choice of the coil

Once the principle it is proved and tested, the magnitude of the magnetic field \mathbf{B} , given a coil diameter, should be defined. The magnitude of \mathbf{B} should be such that it allows the eye to rotate. This means that the forces developed, and thus the net torque acting on the eye is at least 17mNmm to rotate the eye 2^o in any direction (to the left or to the right) compared to the primary position. Figure 6 proves that such torques are feasible. It is obvious that the target is achieved. Moreover, the torques created are large enough to compensate for an increase in the torque demanded for the case the unpredictable torques perturb the rabbit eye.

For small torques it does not really matter which

coil we choose. Figure 7 shows the dependence of the forces on the power level on each coil. The power is independent of the turns, given that the same coils have the same radius and they are kept at a certain same distance away from the magnets. To choose a coil the trade off between the magnetic field created and the temperature because of the ohmic losses need to be taken into consideration. For this reason, we opt for the coil of 400 loops. When the coil is conducted by 1.5A a torque of 180 mNmm can perturb the rabbit eye. Of course, once the distance between the PMs and the coils decreases from the 8mm of the set up the aforementioned value will increase.

To have an insight about the magnitude of the magnetic field itself, the formula which applies for long solenoids can be used:

$$\mathbf{B} = \mu_o \frac{In}{l} \tag{3}$$

,where I is the current conducting the coil, n the number of loops, and l length of the coil. The result is a $|\mathbf{B}| = 0.07 Tesla$. Although this is a very rough approximation, given that neither of our coils can be considered as a long solenoid, yet it is a safe estimation. This value could be used as a reference and starting point in future work where the source of a magnetic field can be replaced by a pair of Helmholtz coils. Such a set up, adjusted adequately, can allow the creation of forces in any desired direction (e.g vertically), in a more handy way.

C Dynamic behavior of the PMs - coil system

From the results presented in Figure 9 it is concluded that the system PMs-Coil is linear.

However, as mentioned earlier, the currents in the coil were too low. This resulted in very small forces that put in question the validity of the results. To guarantee the soundness of the results the experiments must be repeated under different conditions. In the first place, in order to supply the coil with sufficient current (at the magnitudes used in DC experiments), the output of the function generator can be the input to a voltage controlled current source (VCIS). Moreover, the current must be recorded in a way that we can also calculate the phase of the system. For example, once sufficient coil is supplied, a resistor could be placed in series with the coil. If the voltage in the resistor is recorded, we can retrieve the magnitude and phase of the current at each time. Once that is achieved, appropriate synchronization with the measurements of the forces can provide information about the magnitude and phase of the system in a secure way.

D In vivo experiments

The preliminary in vivo experiments were successful. In this first stage it is proven that the actuator works. The next step is to do a calibration, based on the in vitro results, and record the angles that occur. A series of experiments is enabled with the use of the device. For example, the torque angle transfer function of the oculomotor plant can be calculated. Moreover, combined with signals recorded from cerebellum, the role of the latter in oculomotor control can be further studied. Also, recordings from any other oculomotor structure would be interesting.

Acknowledgments

The current study was conducted at the Cerebellar Systems Physiology Group of the Department of Neuroscience in Erasmus Medical Centre (EMC), in the frame of the graduation thesis for the MSc of Biomedical Engineering at TU Delft. It was supervised by F.C.T van der Helm (TU Delft) and A.C.Schouten (TU Delft) and M. Frens (EMC).

Appendix A: Calibration

After calibration the force-voltage relationships were: for sensor 1: $F_1(mN) = 44.95(V) - 173.2$ and for sensor 2: $F_2(mN) = 37.42(V) - 173$, where V was the voltage related to each force.

Appendix B: Magnetic field and forces

The force in a gradient field is given by [13]:

$$\mathbf{F} = grad(\mathbf{m} \cdot \mathbf{B}) \tag{4}$$

, where **m** is the magnetic moment and **B**the magnetic field. Figure 11 shows the force components, grad**B** and the vector **B** when the magnet is rotated by an angle θ .

The following relations hold:

$$|F_z| = |\mathbf{m}||grad\mathbf{B}|\cos\theta \tag{5}$$

$$|F_T| = |\mathbf{F}|\cos\theta\tag{6}$$

$$|F_x| = |\mathbf{F}|\sin\theta\tag{7}$$

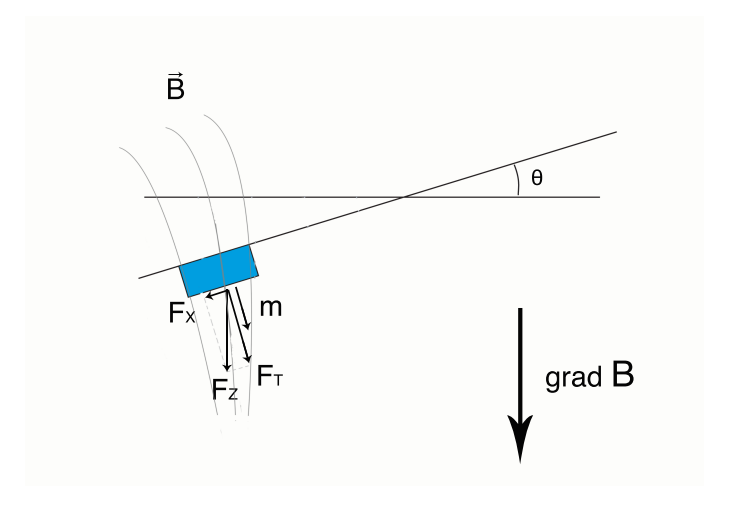


Figure 11: A PM (blue box) under a magnetic field **B**. F_z is the magnetic force, F_x and F_T are the two components of F_z . F_T contributes to the rotation of the eye.

where F_T is the component that will produce the torque. In the first place the $|\mathbf{m}|$ is the same for any orientation. Moreover, we focus on the small angles demanded (up to 2^o). The minimum cosine will be at 2^o and it is $\cos 2^o = 0.9994$, so we can assume that $\cos \theta \simeq 1$ for any rotation between $0 - 2^o$ (and $\sin 2^o = 0.0.03$, so $\sin \theta \simeq 0$) and thus equations 5, 6 and 7, can be rewritten as:

$$|\mathbf{F}| \simeq |\mathbf{m}||grad\mathbf{B}|$$
 (8)

$$|F_T| \simeq |\mathbf{F}|$$
 (9)

$$|F_x| \simeq 0 \tag{10}$$

We expect gradB to be proportional to ${\bf B},$ and that is proportional to the current in the coil. Equations 8 and 9 imply that

$$|F_T| \propto |\mathbf{B}|$$
 (11)

Thus, we can assume that the torque exerted on the ring is proportional to the magnetic field \mathbf{B} .

References

- P. Bach-y Rita and F. Ito. Properties of stretch receptors in cat extraocular muscles. *Journal of Physiology*, 186:663–688, 1966.
- [2] D. Balslev and R.C. Miall. Eye position representation in human anterior parietal cortex.

- The Journal of Neuroscience, 28(36):8968–8972, 2008.
- [3] N.H. Barmack. Measurements of stiffeness of the extraocular muscles of the rabbit. *Journal of neurophysiology*, (39), 1976.
- [4] D.S. Childress and R.W Jones. Mechanics of horizontal movement of human eye. *Journal of Physiology*, (188):273–284, 1967.
- [5] H. Colewijn. The oculomotor System of the Rabbit and its Plasticity. Springer-Verlag, 1981.
- [6] C.C. Collins, M.R. Carlson, A.B. Scott, and A. Jampolsky. Extraocular muscle forces in normal human subjects. *Investigative Ophthalmol*ogy and Visual Science, 20(5):652–664, 1981.
- [7] E. de Vlugt, A.C. Schouten, and F.C.T. van der Helm. Closed-loop multivariable system identification for the characterization of the dynamic arm compliance using continuous force disturbances: a model study. *Journal of Neuroscience Methods*, 122:123–140, 2003.
- [8] I.M. Donaldson. The functions of the proprioceptors of the eye muscles. *Philosophical Transactions, Royal Society London*, (355):1685–1754, 2000.
- [9] T.J. Ebner and S. Pasalar. Cerebellum predicts the future motor state. The Cerebellum, 7(4):583–588, 2008.
- [10] A. Feutsel, O. Krusemark, and J. Mller. Numerical simulation and optimization of planar electromagnetic actuators. Sensors and actuators A, (70):276–282, 1998.
- [11] M. A. Frens and O. Donchin. Forward models and state estimation in compensatory eye movements. Frontiers in Cellular Neuroscience, 3.
- [12] N. Ida and J.P.A. Bastos. *Electromagnetics and calculation of fields*. Springer, second edition, 1997.
- [13] A. Kruusing. Optimizing magnetization orientation of permanent magnets for maximal gradient force. *Journal of Magnetism and Magnetic Materials*, (234):545–555, 2001.
- [14] G. Lennerstrand. Strabismus and eye muscle function. *Acta Ophthalmologica Scandinavica*, (85):711–723, 2007.

- [15] J.R. Lukas, R. Blumer, M. Denk, I. Baumgartner, W. Neuhuber, and R. Mayr. Innervated myotendinous cylinders in human extraocular muscles. *Investigative Ophthalmology and Visual Science*, (41):2422 2431, Aug. 2000.
- [16] S. Pasalar, A.V. Roitman, W.K. Durfee, and T.J. Ebner. Force field effects on cerebellar purkinje cell discharge with implications for internal models. *Nature Neuroscience*, 9(11), 2006.
- [17] D. A. Robinson. The use of control systems analysis in the neurophysiology of eye movements. *Annu Rev Neurosci*, pages 463–503, 1981.
- [18] G. L. Ruskell. The fine structure of human extraocular muscle spindles and their potential proprioceptive capacity. *J. Anat.*, (167):199–214, 1989.
- [19] A.C. Schouten, E. de Vlugt, and F.C.T. van der Helm. Design of perturbation signals for the estimation of proprioceptive reflexes. Biomedical Engineering, IEEE Transactions on, 55(5):1612–1619, 2008.
- [20] R. Shadmehr and J. W. Krakauer. A computational neuroanatomy for motor control. Exp Brain Res, 185:359–381, 2008.
- [21] J.G. Thomas. The torque angle transfer function of the human eye. *Biological Cybernetics*, 3(5):254–263, 1967.
- [22] F.C.T. van der Helm, A.C. Schouten, E. de Vlugt, and G.G. Brouwn. Identification of intrinsic and reflexive components of human arm dynamics during postural control. *Journal of Neuroscience Methods*, 119:1–14, 2002.
- [23] H. van der Kooij, S. Donker, M. de Vrijer, and F. van der Helm. Identification of human balance control in standing. Systems, Man and Cybernetics, 2004 IEEE International Conference on, 3:2535–2541, 2004.
- [24] C.R. Weir. Proprioception in extraocular muscles. J-Neuro-Opthalmol, (26):123–127, 2006.
- [25] B. Winkelman and M. Frens. Motor coding in floccular climbing fibers. *Journal of Neurophysiology*, (95):2342–2351, 2006.
- [26] M. Wnag., X.and Zhang, I.S. Cohen, and M.E. Goldberg. The proprioceptive representation

- of eye position in monkey primary somatosensory cortex. Nature Neuroscience, $10(5):640-646,\ 2007.$
- [27] D.M. Wolpert, Miall C., and Kawato M. Internal models in the cerebellum. *Trends in Cognitive Sciences*, 2(9), 1998.